The Reorganization Energy of Azurin in Bulk Solution and in the Electrochemical Scanning Tunneling Microscopy Setup

Stefano Corni*

INFM Center on nanoStructures and bioSystems at Surfaces (S³), Modena, Italy

Received: September 6, 2004; In Final Form: December 1, 2004

The total reorganization energy λ of azurin is theoretically studied both for the electron self-exchange reaction and for the protein in the electrochemical scanning tunneling microscopy (ECSTM) setup. The results demonstrate the importance of the proximity between the active sites in the encounter complex to reduce λ for the electron self-exchange reaction and quantifies the effects of the presence of an STM environment (tip and substrate) on λ. A comparison of the calculated results with experimental data is performed, and the relative magnitudes of the inner and outer contributions to λ are discussed.

1. Introduction

Azurin (Az) is a protein belonging to the family of cupredoxins. These are redox-active proteins characterized by a type I copper active site,[1] whose natural function is to act as electron transfer (ET) agents in different biochemical redox processes.[2] Az, in particular, seems a good candidate for the implementation of biomolecular electronic devices.[3] Recently, the ability of Az to carry electric current has been probed using an electrochemical scanning tunneling microscopy (ECSTM) approach.[4−6] The theoretical interpretation of such experiments requires calculation of the important properties of the proteins[7] relevant to the specific experimental setup. In Marcus's theory (and in related theories proposed to explain ECSTM data),[8] a key such quantity is the reorganization energy λ. λ is usually divided into two contributions: λ_{in} and λ_{out}. In the case of proteins, the inner reorganization energy λ_{in} refers to the reorganization of the active site; the outer contribution λ_{out} collects terms by the remainder of the protein and by the environment surrounding the protein. On the basis of a simple continuum model,[8b] it has been proposed that the presence of an STM tip and substrate close to the molecule may significantly affect λ_{out} by the replacement of solvent (water) molecules with metal. Here, we report our calculations of λ for the electron self-exchange (ESE) reaction of Az in aqueous solution and for an ET process involved in the ECSTM measurement. In particular, the quantitative effects of the ECSTM setup on λ_{out} will be presented for the first time. For the inner contribution λ_{in}, we shall use the theoretical estimate by Ryde and Olsson,[9] while for λ_{out}, a continuum model will be used in which the active site is treated quantum mechanically, while each of the other portions of the system (the rest of the protein, the solvent, the STM tip, and the STM substrate) is described as a specific continuum dielectric or conductor medium. λ_{out} will be calculated as a difference of nonequilibrium and equilibrium free energies for active-site charge densities proper for the processes under study.

The article is organized as follows: In section 2, the investigated processes are presented together with the model and the methodologies used to calculate λ. In section 3.1, we focus on the results relative to the ESE reaction of Az, while in section 3.2, the results regarding Az in the ECSTM setup are discussed and compared with the experiments by Alessandrini et al.[6] A discussion of the dependence of λ on the ECSTM details is given in section 3.3, and finally in section 4, some conclusions are drawn.

2. Theory

We shall consider two ET processes: one (a) is the ESE reaction of Az, and the other (b) is the ET between a single Az molecule and an electrode (the tip or substrate) in the ECSTM (a schematic is shown in Figure 1).

(a) The reaction for which λ will be calculated is

$$[\mathrm{Az(I)-Az(II)}]_{enc} \rightarrow [\mathrm{Az(II)-Az(I)}]_{enc} \quad (1)$$

where $[\mathrm{Az(I)-Az(II)}]_{enc}$ refers to the encounter complex formed by one reduced Az and one oxidized Az (in $[\mathrm{Az(II)-Az(I)}]_{enc}$, the Az oxidation states are swapped). The geometry of the encounter complex in solution is actually unknown (it is a very labile, short-lived complex). However, the geometry of azurin dimers in the solid state seems to be a reasonable approximation of such a complex (on this point also, see ref 10), because the molecules dock through their hydrophobic patches, and the copper ions are close to each other, maximizing the reaction probability. Thus, the geometry for the complex that will be used in the calculations is the same as in the crystal structure (protein data bank file 4AZU).[11]

(b) In the case of Az in ECSTM, we shall consider the reaction

$$\mathrm{Az(II)} + \mathrm{electrode}[ne^-] \rightarrow \mathrm{Az(I)} + \mathrm{electrode}[(n-1)e^-] \quad (2)$$

In eq 2, "electrode" may refer to the STM substrate or to the tip. We shall assume that the electron of the tip or the substrate that is transferred to Az was delocalized on the whole (macroscopic) volume of the electrode (n in eq 2 is a macroscopic number of particles), and thus, its contribution to the overall variation in the charge density upon the ET in eq 2 is negligible. Hence, the reorganization energy associated with eq 2, which basically depends on such charge density variation, is the same whether "electrode" refers to the tip or to the substrate. As we shall discuss in section 3.2, different theories

* E-mail: corni.stefano@unimore.it.

10.1021/jp0459920 CCC: $30.25
Published on Web 01/27/2005

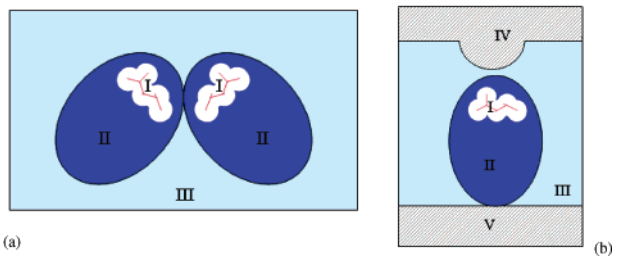

Figure 1. Schematic representations of the models used in the present work: (a) ESE reaction of Az; (b) Az in the ECSTM geometry. The numbering refers to regions with different dielectric properties: I, active site cavity (the atomistic active site, treated quantum-mechanically, is sketched in red); II, protein scaffold; III, solvent; IV, STM tip; V, STM substrate. Drawings are out of scale.

formulated to explain the conduction mechanism of adsorbates in ECSTM[8] call into question the reorganization energy of the same reaction (i.e., eq 2).

Note that two Az molecules participate in eq 1, whereas only one Az molecule is involved in eq 2. To meaningfully compare λ for the two processes, λ should refer to the same number of Az molecules. For this reason, in the following we shall use λ, λ_{in}, and λ_{out} that refer to a single Az molecule (e.g., for reaction 1, we shall consider half the value of the reaction reorganization energy), whatever the ET process and the source of the data (our calculations or the literature).

2.1. Estimate of λ_{in}. In ref 11, the value of λ_{in} for ESE is reported to be 0.146 eV (normalized to a single Az molecule), obtained by using a quantum mechanical/molecular mechanics (QM/MM) technique. In particular, Ryde and Olsson treated the Az active site at the QM (density functional theory, DFT) level, while they exploited an MM description of the rest of the protein. We assume that λ_{in} for the process in eq 2 is the same as for ESE (i.e., we neglect possible effects of the ECSTM environment on λ_{in}).

2.2. The Model to Calculate λ_{out}. The model used to calculate λ_{out} is a generalization of the integral equation formalism (IEF) version[12] of the polarizable continuum model (PCM)[13] and has been implemented in the quantum chemistry code GAMESS.[14] In PCM, originally developed for solutions, a QM description of the solute is coupled to a continuous model of the solvent (PCM has also recently been generalized to various complex systems).[15] In our model, which preserves the basic philosophy of PCM, the active site of the protein is described atomistically at a QM level (DFT in the present work), while the remainder of the system (protein scaffold, solvent, STM tip, and substrate) is represented by different continuous media. The active site is hosted in a molecularly shaped cavity built in the dielectric that represents the protein.

In particular, for the calculations on the ESE reaction in eq 1, the space is partitioned into three regions with different dielectric properties (see Figure 1a): The first region is formed by the two cavities that host the quantum mechanical active sites ($\epsilon = 1$, number I in Figure 1), the second is the dielectric representing the protein (II in Figure 1, characterized by the nonlocal dielectric function discussed in section 2.2.2 for the static response and by a dynamical local permittivity $\epsilon_{pro,dyn} = 2$), and the third is the solvent (water, static permittivity $\epsilon_{sol,stat} = 78.39$, dynamical permittivity $\epsilon_{sol,dyn} = 1.776$, III in Figure 1). A description of how the boundaries between the various regions are defined will be given later. For the protein in the STM configuration (Figure 1b), two other regions are present: the STM tip (IV in Figure 1b) and the substrate (V in Figure 1b). They are treated as perfect conductors with respect to both the static and dynamic responses. We have specified the static and the dynamic dielectric properties of the continuous media, because both are involved in the calculation of λ_{out} (see section 2.3).

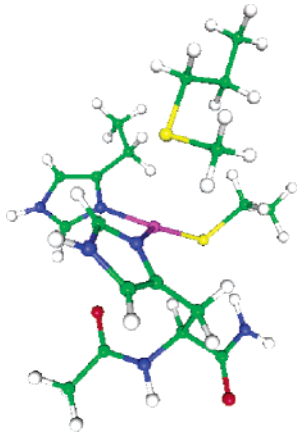

Figure 2. Model active site used in the calculations. Cu = purple, S = yellow, N = blue, O = red, C = green, H = white.

In the following, we shall present in more detail the models used for the various components of the system.

2.2.1. Active Site. A molecule that models the active site has been obtained by pruning the protein as detailed in ref 16. The resulting compound is depicted in Figure 2. DFT has been used to compute the ground-state total energy and electronic structure of the optimized active site, starting from the X-ray geometry (protein data bank file 4AZU, http://pdb.gmd.de). The B3LYP exchange-correlation functional as implemented in the quantum chemistry program GAMESS and the 6-31G* basis set were used. The geometry of the active site was obtained by energy minimization, as described in ref 16. The cavity that hosts the active site was built as a union of interlocking spheres placed on each atom of the active site. The radii of such spheres were the van der Waals radii multiplied by a factor of 1.4, intermediate between the values suitable for highly and low polar dielectric solvents,[17] as the protein medium surrounding the active site can be considered. Tests performed with a factor of 1.2[18] showed negligible variations of λ_{out}. The resulting boundary of the cavity used in the calculation is the red contour in Figure 3.

2.2.2. Protein Scaffold. The protein outside the active site has been considered a homogeneous dielectric having a finite size and a complex shape. The overall shape of this dielectric was designed as an approximation of the protein molecular surface, obtained as the surface of a union of interlocking spheres centered on the Cα of each amino acid. All of the spheres had the same radius. This was chosen by imposing the condition that the volume of the sphere union be equal to the molecular volume of the protein, calculated via the GEPOL procedure[19] as implemented in *Gaussian 98*.[20] The resulting surface of the protein is the union of the solvent-exposed portion of the sphere surface. The protein shapes used in the calculations are depicted in Figure 3 (blue contours).

A nonlocal dielectric constant was used for the static response of the protein, allowing us to include a different screening for long-range and short-range Coulombic interactions. In particular, the simple single-pole form given in ref 21 has been exploited:

$$\frac{1}{\epsilon_{pro}(k)} = \frac{1}{\epsilon_{pro,s}} + \left(\frac{1}{\epsilon_{pro,l}} - \frac{1}{\epsilon_{pro,s}}\right)\frac{1}{1+\Lambda^2 k^2} \qquad (3)$$

where $\epsilon_{pro}(k)$ is the protein constant in the reciprocal space, $\epsilon_{pro,l}$

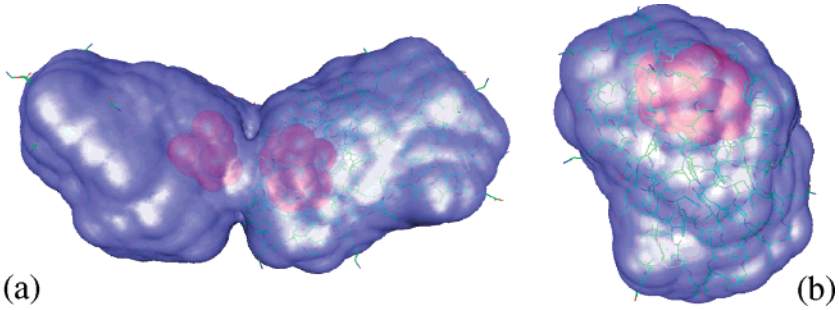

Figure 3. Protein shapes used in the calculations for (a) the ESE reaction of Az, eq 1, and (b) a single Az molecule (as in eq 2). The boundary between the protein and the solvent is represented in blue, the one between the active site cavity and the protein is red.

is the dielectric constant for long-range Coulombic interactions, and $\epsilon_{pro,s}$ is the dielectric constant for short-range Coulombic interactions. Short-range and long-range are defined with respect to the correlation length Λ. It is worth mentioning that the simple Lorentzian form given in eq 3 is known to be a poor representation of the nonlocal response of liquid solvents,[22] for which more advanced approaches have been proposed.[23] However, much less is known on the nonlocal dielectric response of proteins, and eq 3 surely catches one aspect of the protein response (i.e., the different screening capability for short range and long-range Coulombic interactions). In addition, Basilevsky and Parsons[24] have demonstrated that, even for homogeneous solutions, a rigid cavity continuum model (as ours) together with a Lorentzian dielectric constant as in eq 3 reproduces the solvation energy results of a more advanced model employing a nonrigid cavity and the correct nonlocal dielectric response for the solvent.

Let us now discuss the choice of the parameters that enter $\epsilon_{pro}(k)$ in eq 3. Short-range interactions are basically screened by the electronic polarization of the medium, thus we have chosen for $\epsilon_{pro,s}$ a typical value for optical dielectric constant, 2. Coherently, we have also used this value for the protein dynamic response $\epsilon_{pro,dyn}$ (considered to be local). The value assumed for $\epsilon_{pro,l}$ (=20) is a typical value for a moderately polar environment, which is what a long-range interaction in a protein should probe. Tests performed with $\epsilon_{pro,l}$ between 4 and 50 manifested small changes on λ_{out} that do not change the conclusions reported in the present article. Finally, we have chosen Λ to be 5 Å, a reasonable value that gives λ_{out} in the same range as the typical local dielectric constants chosen for proteins (i.e., 2−4). The influence of these parameters on the calculated λ value is discussed in section 3.1.

2.2.3 Solvent. The solvent (water in our calculations) is a continuous medium that fills the space not occupied by the other components of the system. Tabulated values of the water permittivity (static, 78.39; dynamic, 1.776) were used. No ionic force effects on λ have been included in our model: a test performed on a simpler model (protein described as a sphere with a spherical cavity containing only the copper ion) by using the linearized Poisson−Boltzmann equation showed that, for the ionic force used in the ECSTM experiments[6] (50 mM), such effects are negligible.

2.2.4. STM Apparatus. The STM substrate is described as a semi-infinite perfect conductor with a planar surface. The tip (also treated as a conductor) is a hemisphere protruding from the planar surface of a conductor. The static and dynamic dielectric responses of a perfect conductor are equal, implying that the tip and the substrate have no slow degrees of freedom that must reorganize upon ET. Thus, they do not give a direct contribution to the reorganization energy. However, this does not mean that they behave like a vacuum: the electric field distribution in the remainder of the system is affected by the different boundary conditions. Hence, the reorganization energy is different as well. Moreover, the electrostatic potential due to the polarization of the tip and substrate ("image" potential) enters into the self-consistent DFT determination of the active-site electronic density (see section 2.3).

2.2.5. Interactions Between the Components. The interaction considered in the model between the active site and the remainder is electrostatic in nature: the charge density of the active site polarizes the surrounding media, thus creating an electric field (reaction field) that acts back on the active site. In our model, the charge density of the active site is obtained by self-consistently taking into account such a reaction field (also called image field in the STM framework). This point will be more deeply discussed in the next section and in Appendix A.

2.3. Procedure to Calculate λ_{out}. Let us consider a given ET reaction (e.g., eq 1 or eq 2) taking place in an environment described as a (possibly multizone) dielectric and leading from the reactants R to the products P, both quantum-mechanically described. The total (electronic plus nuclear) density of charge of R and P will be called ρ_R and ρ_P, respectively. For example, in the case of the ESE reaction, eq 1, ρ_R is the density of charge of the two active sites, one reduced and the other oxidized, while ρ_P is the density of charge of the same active sites with the oxidation states swapped. For eq 2, ρ_R is the charge density of the oxidized active site, while ρ_P is that of the reduced active site. Exactly as for homogeneous solutions,[25,26] the charge densities ρ_R^{eq} and ρ_P^{eq} (i.e., the R and P charge densities equilibrated to the polarization induced by the charge densities themselves) are obtained by minimizing an equilibrium free-energy functional $\mathcal{G}_{eq}[\rho_{R/P}]$ defined as

$$\mathcal{G}_{eq}[\rho_{R/P}] = E[\rho_{R/P}] - \frac{1}{2}\int \rho_{R/P} \cdot V[\rho_{R/P}] \qquad (4)$$

where the integrals are performed over the space occupied by $\rho_{R/P}$, $E[\rho_{R/P}]$ is the vacuum-like energy of the active site calculated for the density $\rho_{R/P}$ (in this work, we use DFT to express it), and $V[\rho_{R/P}]$ is the potential associated with the reaction field (i.e., the electric field due to the polarization induced in the environment by $\rho_{R/P}$). It is worth mentioning that the form of eq 4 does not depend on either the number of different dielectric media considered in the model or the local or nonlocal nature of their dielectric responses. They only have to be linear dielectrics. What obviously depends on the number and nature of the dielectrics is the reaction field potential $V[\rho_{R/P}]$. To calculate such a reaction field, the Poisson equation for the overall system must be solved by using $\rho_{R/P}$ as the source term and by imposing the usual electrostatic boundary conditions at the various interfaces of the system (active site cavity/protein, protein/solvent, solvent/tip, solvent/substrate). In the present

work, we have tackled this problem by using the IEF,[12] which allows rewriting of the differential Poisson equation as a set of integral equations defined only on the boundaries between the various dielectric zones of the system. A boundary element method (BEM) has been used to numerically solve such integral equations. By exploiting these techniques, $V[\rho_{R/P}]$ is finally expressed as the potential produced by a set of apparent point charges placed on the surface of the cavity(ies) hosting the active site(s). Details on the calculation of $V[\rho_{R/P}]$ are given in Appendix A. We remark that BEM has been already applied to the calculation of reorganization energy for ET in proteins,[27] but it has not been coupled to a QM description of the donor/acceptor sites.

$\mathcal{G}_{eq}$ in eq 4 has been minimized with the self-consistent field procedure already described in the literature,[25,26] easily adapted to DFT, leading to ρ_R^{eq}, ρ_P^{eq}, and to the values of $\mathcal{G}_{eq}[\rho_R^{eq}]$ and $\mathcal{G}_{eq}[\rho_P^{eq}]$. These quantities are the first ingredients to calculate λ_{out}.[25,28] The other ingredients are proper *nonequilibrium* free energies[29] ($\mathcal{G}_{neq}$). In particular, we need $\mathcal{G}_{neq}[\rho_P^{neq}, \rho_R^{eq}]$, which means that (a) the charge density is that proper for the P state (we call this density ρ_P^{neq}, the precise definition is given in the following), (b) the environmental polarization related to the slow degrees of freedom of the dielectric media is kept fixed to that induced by ρ_R^{eq}, and (c) the polarization related to the fast degrees of freedom is equilibrated with ρ_P^{neq}. We also need $\mathcal{G}_{neq}[\rho_R^{neq}, \rho_P^{eq}]$, which is analogous to $\mathcal{G}_{neq}[\rho_P^{neq}, \rho_R^{eq}]$ with the roles of R and P exchanged. In the following, we refer only to $\mathcal{G}_{neq}[\rho_P^{neq}, \rho_R^{eq}]$, because the discussion for $\mathcal{G}_{neq}[\rho_R^{neq}, \rho_P^{eq}]$ is the same once R and P are swapped. The expression of $\mathcal{G}_{neq}[\rho_P^{neq}, \rho_R^{eq}]$ is

$$\mathcal{G}_{neq}[\rho_P^{neq}, \rho_R^{eq}] = E[\rho_P^{neq}] + \frac{1}{2}\int \rho_P^{neq} \cdot V_{fast}[\rho_P^{neq}] + \int \rho_P^{neq} \cdot V_{slow}[\rho_R^{eq}] - \frac{1}{2}\int \rho_R^{eq} \cdot V_{slow}[\rho_R^{eq}] \quad (5)$$

$V_{fast}[\rho_P^{neq}]$ is the reaction potential due to the polarization, induced by ρ_P^{neq}, of the fast degrees of freedom of the system surrounding the active sites, while $V_{slow}[\rho_R^{eq}]$ is the analogous quantity for the slow degrees and ρ_R^{eq}. For ET reactions, the fast degrees of freedom are the electronic ones, while the slow degrees of freedom are basically the nuclear ones (vibrations, rototranslations, etc.). The fast degrees of freedom are related to the *optical* dielectric response of the various continuous media surrounding the active site, while the slow degrees of freedom are involved only in the *static* dielectric response. $V_{fast}[\rho_P^{neq}]$ is calculated by the same procedure described in Appendix A for $V[\rho]$, but the *dynamic* (instead of static) dielectric functions of the various continuous media are used. $V_{slow}[\rho_R^{eq}]$ is obtained as the difference of $V[\rho_R^{eq}] - V_{fast}[\rho_R^{eq}]$. ρ_P^{neq}, and then, the value of $\mathcal{G}_{neq}[\rho_P^{neq}, \rho_R^{eq}]$ is obtained by minimizing $\mathcal{G}_{neq}[\rho_P^{neq}, \rho_R^{eq}]$ with respect to ρ_P^{neq} itself. The effective Kohn−Sham equations resulting from the minimization of $\mathcal{G}_{neq}$ and the procedure to solve them are very similar to the corresponding Hartree−Fock ones, which have already been described.[25,30] A general expression of $\mathcal{G}_{neq}$ in terms of the apparent point charges used to calculate V_{fast} and V_{slow} can be found in ref 31, where the subscripts "d" and "in" were used instead of "fast" and "slow". From the knowledge of $\mathcal{G}_{neq}[\rho_P^{neq}, \rho_R^{eq}]$, $\mathcal{G}_{neq}[\rho_R^{neq}, \rho_p^{eq}]$, $\mathcal{G}_{eq}[\rho_R^{eq}]$, and $\mathcal{G}_{eq}[\rho_P^{eq}]$, two reorganization energies λ_{out} can be calculated: One is $\lambda_{out,R} = \mathcal{G}_{neq}[\rho_R^{neq}, \rho_P^{eq}] - \mathcal{G}_{eq}[\rho_R^{eq}]$, and it is related, in the Marcus picture of the ET, to the curvature of the parabola of the reactant state; the other is $\lambda_{out,P} = \mathcal{G}_{neq}[\rho_P^{neq}, \rho_R^{eq}] - \mathcal{G}_{eq}[\rho_P^{eq}]$, which is related to the curvature of the parabola of the product state. In our calculations, we found a small difference between $\lambda_{out,R}$ and $\lambda_{out,P}$ (a few meV), and thus, we considered only a mean value, $\lambda_{out} = (\lambda_{out,R} + \lambda_{out,P})/2$.

TABLE 1: Calculated Az Reorganization Energies for the Electron Self-Exchange (ESE) Reaction, Eq 1, and the Molecule in the ECSTM Setup, Eq 2

	λ_{in} (eV)	λ_{out} (eV)	λ (eV)
ESE eq 1	0.146	0.18	0.33
ECSTM eq 2	0.146	0.29	0.43

When the differences of $\rho_{R/P}^{neq} - \rho_{R/P}^{eq}$ are neglected, λ_{out} can be directly expressed in terms of the charge density difference $\Delta\rho_{PR} = \rho_P^{eq} - \rho_R^{eq}$ as[25]

$$\lambda_{out} = \mathcal{G}_{eq}^{fast}[\Delta\rho_{PR}] - \mathcal{G}_{eq}[\Delta\rho_{PR}] \quad (6)$$

where $\mathcal{G}_{eq}^{fast}$ has the same expression as $\mathcal{G}_{eq}$ in eq 4 with V replaced by V_{fast}. We compared the difference between λ_{out} from eq 6 and λ_{out} from the difference of $\mathcal{G}_{neq} - \mathcal{G}_{eq}$ for two selected processes (ESE for two Az infinitely apart in bulk solution and the ECSTM process in eq 2). We found small discrepancies, in the range of 5 meV. Because the use of eq 6 allows saving two self-consistent field calculations (those needed to find ρ_P^{neq} and ρ_R^{neq}) per each computed λ_{out}, the calculations presented in section 3 have been performed by exploiting such a relationship.

3. Results

3.1. Electron Self-Exchange (ESE) Reaction of Azurin. The λ_{out} value that we calculated for the ESE reaction, eq 1, was 0.18 eV as reported in Table 1. Such a value, together with $\lambda_{in} = 0.146$ eV, gives a total reorganization energy $\lambda = 0.33$ eV (we remind the reader that throughout this article λ will be normalized to a single Az molecule). Because some parameters of the model (in particular, those related to the protein dielectric constant) are not precisely known, we have also estimated the range of calculated values of λ that correspond to reasonable choices of such parameters ($4 \le \epsilon_{pro,l} \le 50$; $1.8 \le \epsilon_{pro,s} = \epsilon_{pro,dyn} \le 2.2$; 2 Å $\le \Lambda \le 10$ Å). We found that $\lambda \approx 0.33 \pm 0.03$ eV. We remark that the uncertainty expressed by this $\pm$ notation does not refer to any claimed accuracy with respect to experimental data; it is only a compact way to express how much the calculation parameters affect the final result. In any case, our calculated λ is in good agreement with the experimental estimate of λ given by Gray and co-workers, 0.3−0.4 eV.[32] Remarkably, both λ_{in} and λ_{out} contribute to λ to similar extents ($\lambda_{in}/\lambda_{out} = 0.81$).

When the inertial response of the protein is completely neglected (i.e., when we assume $\epsilon_{pro,l} = \epsilon_{pro,s} = \epsilon_{pro,dyn} = 2$), only the solvent directly contributes to the outer reorganization energy. In this case, the calculated λ_{out} read 0.15 eV, to be compared with 0.18 eV including the inertial protein response. Although we cannot strictly decompose λ_{out} into protein scaffold and solvent contributions (their polarizations mutually affect each other), these results show that most of the λ_{out} for eq 1 is to be ascribed to the solvent.

The value of λ_{out} given already (0.18 eV) is calculated for the encounter complex geometry. λ_{out} for two Az molecules infinitely apart in solution is much larger (i.e., 0.40 eV). The increase of the reorganization energy when the donor−acceptor distance increases is a well-known feature of ET in solution, and it is also predicted by the simple two-sphere continuum model originally proposed by Marcus.[28] In fact, when the donor and the acceptor come closer together, the former tends to be immersed in the polarized environment induced by the latter, and vice versa. Thus, the ET reactants feel before the ET an environmental polarization which is already partly adapted to

the ET products. In other words, the extent of the required environmental reorganization decreases, and so does the reorganization energy. However, another reason might cause this trend in λ_{out} for the studied system. In fact, the presence of a second protein in the encounter complex removes water from the neighborhood of the first one, and thus it removes an effective source of reorganization energy. To check if this solvent exclusion phenomenon really affects λ_{out}, we performed a calculation on a fictitious encounter complex with one of the two active sites removed. ρ_R in this case is the charge density of the survived active site in the reduced form, while ρ_P is the charge density for the same site in the oxidized form. For this system, only the water removal effect is active in reducing λ_{out}. If the difference depended on water removal, λ_{out} should be equal to that of the encounter complex (i.e., 0.18 eV). We instead obtained 0.39 eV, close to the value for the isolated proteins (0.40 eV). Thus, the large effects of the protein−protein distance on the ET is not related to water removal, but only to the relative closeness between the two active sites in the encounter complex (Cu−Cu distance of approximately 15 Å). The importance of the active-site proximity in protein−protein ET is usually thought to relate to the need for a good electronic coupling, but our findings show that in the present case active-site proximity can also affect ET kinetics through effects upon reorganization energy.

3.2. Reorganization Energy of Azurin in the Electrochemical STM Configuration. The calculation for the protein in the ECSTM, eq 2, has been done by assuming an STM tip radius of 5 nm. The protein stands with its major axis of inertia perpendicular to the substrate. The Cys3/Cys26 disulfide bridge is close to the substrate surface. The tip is 5 Å from the protein surface, a reasonable value for STM in solution. These details of the STM configuration were chosen to be as close as possible to a precise experiment.[6] In this geometrical arrangement, the computed value of λ_{out} is 0.29 eV (±0.04 eV due to the uncertainties on the protein dielectric constant), giving $\lambda = 0.43$ eV. To obtain an estimate of λ from experimental data, Alessandrini et al.[6] had to assume a mechanism for the electron transport through the protein. When the resonance tunneling model[8a] was used to fit the experimental data, λ resulted to be 0.13 eV. By fitting the vibrationally coherent model[8b] to the experiments, the result was $\lambda = 0.53$ eV instead. We remark that, although the resonance tunneling model of ref 8a and the vibrationally coherent model of ref 8b represent two different mechanisms for the transfer of electrons between the tip and the substrate via an adsorbate, the reorganization energy that appears in the two models refers to the same ET reaction, eq 2 (i.e., the transfer of one electron from the tip (or from the substrate, no difference in λ) to Az). At first sight, it might appear strange that this particular λ is involved in a resonance tunneling mechanism, because during the resonant tunneling, the charge carrier is never really localized on the molecule, while in eq 2, the electron localizes on the protein in the product state. However, λ for eq 2 is not only a measure of the reorganization when ET really takes place, but it can also be interpreted as the difference between the energy of the molecular level available for the incoming charge (i.e., the level that matters in resonant tunneling) and the energy corresponding to the standard redox potential E^0 of the molecule (basically, this is part of Gerischer's picture of the ET).[33,34] Thus, λ appears in the expression of the resonant tunneling rate when the energy of the molecular level available for tunneling (an unknown quantity) is expressed in terms of E^0 (a known quantity).[8a] There is also another reason that makes the resonant tunneling rate dependent on λ: λ for eq 2 is also a measure of the *thermal fluctuations* of the energy of the available level of the molecule. The ECSTM experiment does not probe a single ET event, but a great number of them (the time scale of the measurement of the current is much longer than the time scale of the single ET). For each ET event, the energy of the available molecular level will be different because of fluctuations. When an average rate is taken, the typical extent of the fluctuation (related to λ of eq 2) appears in the equations.[8a] In any case, by comparing our calculated result ($\lambda = 0.43$ eV) for the reaction in eq 2 with the reorganization energies found in ref 6, the resonance tunneling mechanism seems to be an improbable explanation of this ECSTM experiment, since it gives too small a value for λ, 0.13 eV.

Let us now compare the calculated λ values for ESE and ECSTM. We note that λ in the ECSTM geometry (0.43 eV) is larger than λ for the ET in eq 1, 0.33 eV. To understand the origin of this difference, we can consider a number of steps that lead from the process in eq 1, the ESE reaction, to the process in eq 2, the ET in the ECSTM. At each step, there is a change in the considered ET process and thus a variation in λ. The total λ variation in passing from eq 1 to eq 2 is thus decomposed into step contributions (see the scheme in Figure 4). We considered three steps:

1. The two Az molecules forming the encounter complex (Figure 3a) are divided and moved away to infinite distance in bulk solution. The reorganization energy variation of the first step, referring to one Az molecule as usual, reads $\Delta\lambda_1 = 0.22$ eV (i.e., λ increases). As noted in section 3.1, this is due to the loss of proximity of the active sites in the encounter complex, which reduces the need for reorganization.

2. One of the two Az molecules is replaced by the ECSTM apparatus, keeping the other Az far from it, in bulk solution. After this change, the considered process is an ET between one Az molecule and an infinitely distant electrode (tip or substrate). By considering that the two ET partners (two Az's before this step, one Az and the ECSTM electrodes after the step) are too far to affect each other and that the ECSTM apparatus does not bring any direct contribution to λ (its charge variation upon ET is negligible), the reorganization energy referring to one Az molecule is the same before and after the present step (i.e., $\Delta\lambda_2 = 0$).

3. In the third step, the Az molecule is taken from the bulk solution and placed in the ECSTM setup, in the position for which λ for eq 2 has been calculated. For this step, $\Delta\lambda_3 = -0.12$ eV. Such a decrease of λ is due to the water removal effects (as already pointed out in ref 8b): some of the water that surrounds the molecule in bulk solution is replaced by the STM tip and the substrate in the ECSTM geometry. While water can give a large contribution to λ_{out} for the protein, the tip and the substrate do not.

Obviously, the total variation of λ (normalized to a single molecule) between ESE and ECSTM is the algebraic sum of $\Delta\lambda_1$, $\Delta\lambda_2$, and $\Delta\lambda_3$. Such a total variation (even its sign) cannot be determined a priori by intuitive arguments. In fact, it depends on two opposing effects with similar magnitude: on one hand, the presence of the ECSTM apparatus removes water from the protein neighborhood, decreasing λ_{out}; on the other hand, the reduction of λ_{out} in the encounter complex due to the active-site closeness is lost in the ECSTM process. In the present case, the latter effect prevails over the former ($|\Delta\lambda_1| > |\Delta\lambda_3|$), and the overall $\Delta\lambda$ is positive.

3.3. Dependence of λ_{out} on the ECSTM Configuration Details. The value of λ_{out} depends, in general, on the environmental details. Thus, to compare calculated values with experi-

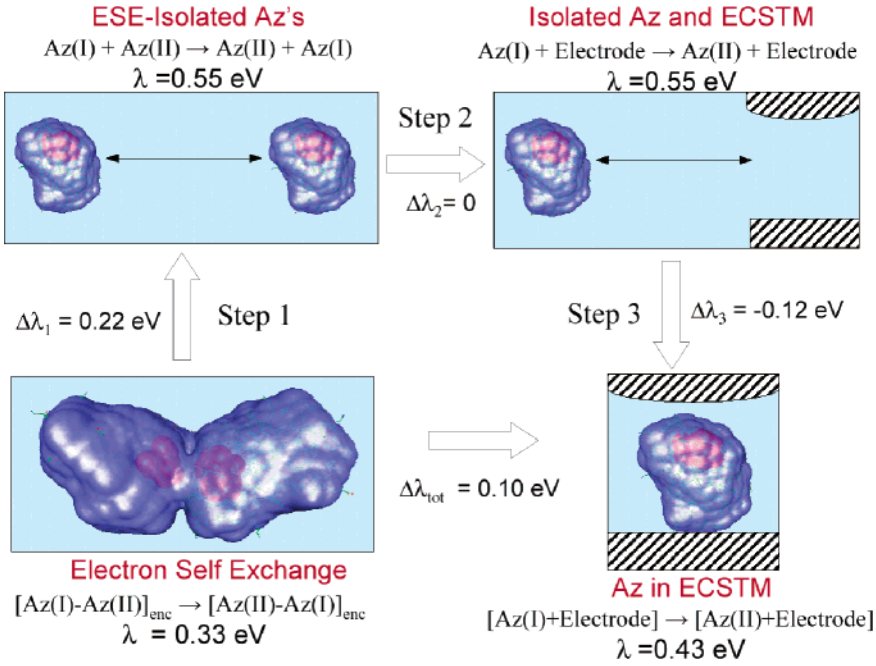

Figure 4. Decomposition of the reorganization energy difference between the reaction in eq 1 (electron self-exchange) and that in eq 2 (Az in ECSTM) in step contributions. All the values of reorganization energy refer to a single Az molecule, which explains why $\Delta\lambda_2 = 0$.

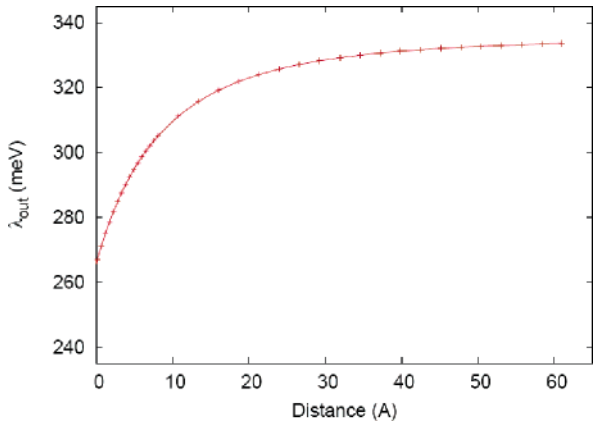

Figure 5. Calculated λ_{out} as a function of the tip−protein distance.

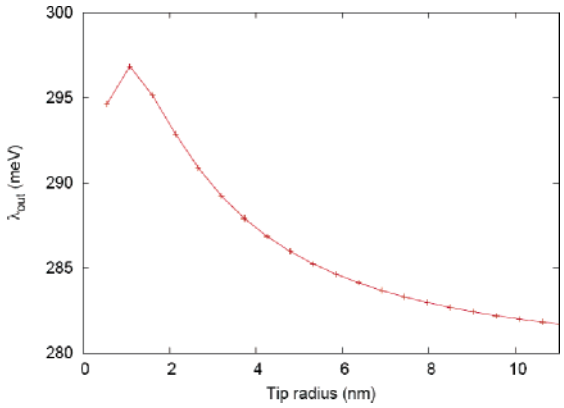

Figure 6. Calculated λ_{out} as a function of the tip radius.

mental ones, one should reproduce the experimental system in the calculations as accurately as possible. Unfortunately, not all the (reasonably mattering) details are known for the experiment of ref 6, to which we want to compare. In particular, as in most STM studies (especially those performed in solution), the distance of the tip from the substrate is unknown, as well as the detailed shape and size of the microscopic portion of the tip that really acts as the electron drain in the STM measurements.[35] To check how these setup details affect the value of λ_{out} and to verify if the conclusions reported in this article are robust with respect to reasonable changes in these parameters, we have calculated λ_{out} for a range of tip−protein distances and tip radii. The results are reported in Figures 5 and 6, respectively.

Note that, in Figure 5, the reorganization energy decreases by decreasing the tip−protein distance, because more solvent molecules are replaced by the tip. Because of the exponential decay of the STM current as a function of the tip−molecule distance, only tip−protein distances smaller than approximately 10 Å can give measurable currents. In this distance range, λ_{out} changes from 0.27 to 0.31 eV, that is, the total value of λ ranges between 0.41 and 0.45 eV (which is comparable to the uncertainty due to the protein dielectric parameters). Our conclusions are not affected by these changes. The effects of the tip size are even less important: by changing the tip-radius from 0.5 to 10 nm, λ varies less than 0.02 eV. As expected, the reorganization energy increases as the tip becomes smaller, because the solvent exclusion effect is reduced. Note however that, for very small tips, λ_{out} should again approach the large tip-radius limit, because the microscopic bump that constitutes the tip in our model tends to disappear and be replaced by the macroscopic remainder of the tip, which has an almost flat surface (on the protein length scale). This is the reason for the maximum that can be observed in Figure 6 for a radius of approximately 1 nm.

Another parameter that may affect λ_{out} is the orientation of the protein with respect to the substrate. Although the AFM protein height seems to confirm that azurin stands up on the substrate,[35] we have nevertheless calculated the effects of possible changes in the protein orientation under STM measurement conditions, also taking into account possible effects due to the confinement between the tip and the substrate on the water dielectric constant. In particular, we have tried to give a lower boundary estimate of λ for Az in ECSTM setup. To this end,

we have considered the protein lying with its major axis parallel to the substrate, with the tip almost touching the molecular surface (tip−substrate distance: 29 Å). As for the confinement effect on the dielectric constant of water, a recent work[36] suggests that for water confined between two layers ~30 Å apart, the static dielectric constant is around 10−20. We have used the most conservative value of this range, 10. With these assumptions, for eq 2, we obtained $\lambda_{out} = 0.20$ eV (i.e., $\lambda = 0.35$ eV), which is smaller than the isolated Az λ_{out} and comparable to the value for the encounter complex. In this case, the decrease in λ_{out} due to the water removal compensates the increase due to the removal of the second protein. Remarkably, this lower boundary estimate of λ is still larger than the experimental value obtained by assuming a resonance tunneling mechanism for the electron transport through the protein (0.13 eV). Only invoking other effects, such as the possible squeezing of the protein during the STM measurement (that would probably change also λ_{in}) or the nonlinear dielectric response effects for the solvent/protein due to the relatively high electric field in the tip−substrate gap, the computation might be reconciled with the experimental resonance tunneling result. Work on these points is ongoing in our lab. However, on the basis of the results of the present work, a purely resonance tunnel mechanism for conduction through Az appears, at least, unlikely.

4. Conclusions

In this article, a computational model for the evaluation of outer reorganization energies for proteins in bulk solutions and in the ECSTM setup has been presented and applied to Az. The model is based on an accurate (quantum mechanical) description of the protein active site coupled to a continuum description of the remainder of the system (protein scaffold, solvent, STM apparatus). Different findings have been pointed out:

1. For the ESE reaction, λ is strongly affected by the proximity of the two active sites. In particular, such proximity reduces the value of λ with respect to two Az molecules well-separated in solution.

2. The difference in λ between the ESE reaction and the ECSTM process (both normalized to a single Az molecule) can hardly be guessed without detailed calculations, because it depends on two effects (related to water removal due to the STM apparatus and to the active site proximity) giving contributions to λ of similar magnitude but with opposite sign. For the particular case studied in this article, the λ_{ESE} normalized to a single molecule is larger than λ_{ECSTM}.

3. The comparison between the ECSTM reorganization energy calculated in the present work and the ones obtained from the experiment of Facci and co-workers[6] seems to disfavor an explanation of the Az transport properties based on a pure resonance tunneling.

4. Both λ_{in} and λ_{out} similarly contribute to the total reorganization energy λ. The precise interplay between the two depends on the specific process under study ($\lambda_{in}/\lambda_{out} = 0.81$ for ESE and $\lambda_{in}/\lambda_{out} = 0.52$ for ECSTM).

Appendix A

As stated in section 2.3, the reaction potential $V(\rho_{R/P})$ is obtained by solving the Poisson equation via an integral equation formalism (IEF) that allows one to rewrite the differential Poisson equation as a set of integral equations defined on the boundaries between the various dielectrics in the system. Each integral equation involves integral operators defined in terms of the Green's functions of the two regions separated by the interface. Such equations give as a result an apparent surface density of charge σ placed on the boundaries. σ is such to give origin to the required reaction potential $V[\rho_{R/P}]$.[12] A strong point of IEF, besides the reduction of a 3D problem to a 2D one, becomes apparent when a Green's function that takes into account the proper boundary conditions for a given interface is available. In this case, the integral equation on that interface is identically verified, and the interface is not to be explicitly considered in the calculations anymore. This property of IEF has already been exploited to calculate, for example, excitation energies and fluorescence lifetimes of molecules close to nonlocal metals with rough, planar surfaces or spherical nanoparticles.[37] In the present work, we exploited this property as well, because the boundary conditions at the tip−solvent and tip−substrate interfaces are taken into account by a Green's function that contains image charge contributions. The presence of two conductor/dielectric interfaces would require summing an infinite series of images,[37b] corresponding to consecutive reflections of the images in one conductor (say, the tip) into the other (say, the substrate), and vice versa. We found that truncating the sum to 50 reflections gave a good approximation to the true Green's function. Thus, we are left with only two interfaces: active-site cavity/protein and protein/solvent. To solve the integral equation defined on these boundaries, we applied a boundary element method (BEM) (i.e., we discretized each boundary into small portions, called tesserae). The apparent surface charge density σ is consequently discretized into a set of point charges $\mathbf{q}$, each placed in the center of a tessera, and the integral equations become matrix equations.

We formulated the integral equation problem in such a way that only the charges $\mathbf{q}$ placed on the interface between the cavity and the protein are needed to calculate $V(\rho_{R/P})$. For this interface, the matrix equation is

$$[\mathbf{S}^{Out}(2\pi\mathbf{I} + \mathbf{D}^{Cav*}) + (2\pi\mathbf{I} - \mathbf{D}^{Out})\mathbf{S}^{Cav}]\mathbf{A}^{-1}\mathbf{q} = \mathbf{S}^{Out}\mathbf{E}_\rho - (2\pi\mathbf{I} - \mathbf{D}^{Out})\mathbf{V}_\rho \quad \text{(A1)}$$

where $\mathbf{S}^{Out}$ and $\mathbf{D}^{Out}$ are the matrices built from the Green's function of the space outside the cavity, called $G^{out}(\mathbf{r}, \mathbf{r}')$, while $\mathbf{S}^{Cav}$, $\mathbf{D}^{Cav}$, and $\mathbf{D}^{Cav*}$ are matrices built from the empty-space Green's function, $1/|\mathbf{r} - \mathbf{r}'|$ (how these matrices are built from the proper Green's function is described, for example, in ref 12c). In eq A1, $\mathbf{A}$ is the diagonal matrix collecting the tessera areas, $\mathbf{I}$ is the identity matrix, $\mathbf{V}_\rho$ is a vector collecting the electrostatic potential generated by the active-site density ρ measured in the tessera centers, and $\mathbf{E}_\rho$ is another vector that collects the normal-to-the-surface component of the dielectric displacement generated by ρ in the tessera centers. To find $\mathbf{q}$ from eq A1, we first have to build $\mathbf{S}^{Out}$ and $\mathbf{D}^{Out}$ (i.e., we need $G^{out}(\mathbf{r}, \mathbf{r}')$). $G^{out}(\mathbf{r}, \mathbf{r}')$ is the sum of two parts. One is $G^{pro}(\mathbf{r}, \mathbf{r}')$ (i.e., the Green's function of an infinite, homogeneous dielectric medium having the dielectric response properties of the protein, that is, eq 3). This part, however, does not take into account the boundary conditions at the protein/solvent interface. The other part of $G^{out}(\mathbf{r}, \mathbf{r}')$, called $G^{bound}(\mathbf{r}, \mathbf{r}')$, is needed to account for such conditions. To find it, we have considered the following:

(a) To build $\mathbf{S}^{Out}$ and $\mathbf{D}^{Out}$, we do not need the values of $G^{out}(\mathbf{r}, \mathbf{r}')$ for generic $\mathbf{r}$ and $\mathbf{r}'$; we only need $G^{out}(\mathbf{s}, \mathbf{s}')$, where $\mathbf{s}$ and $\mathbf{s}'$ are the centers of two tesserae.

(b) $G^{out}(\mathbf{r}, \mathbf{r}')$ can be interpreted as the electrostatic potential produced in $\mathbf{r}$ by a unitary charge placed in $\mathbf{r}'$. This is given by the potential produced in $\mathbf{r}$ by assuming an infinite homogeneous medium (i.e., $G^{pro}(\mathbf{r}, \mathbf{r}')$) plus a term due to the boundary (i.e., $G^{bound}(\mathbf{r}, \mathbf{r}')$).

(c) The situation described at the previous point is exactly the same as that leading to eq A1, that is, we have in both cases a source of electric field (the unitary charge placed in $\mathbf{r}'$ versus the active-site density ρ), a boundary between two dielectric regions (the protein/solvent boundary versus the cavity/protein one), an electrostatic potential in a generic $\mathbf{r}$ computed for an homogeneous and infinite medium ($G^{\mathrm{pro}}(\mathbf{r}, \mathbf{r}')$ versus $\int d\mathbf{r}'' \rho(\mathbf{r}'')/|\mathbf{r} - \mathbf{r}''|$) and a contribution to the potential in $\mathbf{r}$ due to the presence of a boundary ($G^{\mathrm{bound}}(\mathbf{r}, \mathbf{r}')$ versus the potential generated in $\mathbf{r}$ by the apparent charges $\mathbf{q}$).

If the analogies pointed out here are exploited, the value of $G^{\mathrm{bound}}(\mathbf{s}, \mathbf{s}')$ in a given tessera center $\mathbf{s}$ can be obtained as the potential produced in $\mathbf{s}$ by a set of point charges $\mathbf{q}_{\mathbf{s}'}{}^{\mathrm{bound}}$, placed on the protein/solvent interface. Such $\mathbf{q}_{\mathbf{s}'}{}^{\mathrm{bound}}$ solves the equation (analogous to eq A1)

$$[\mathbf{S}^{\mathrm{Sol}}(2\pi\mathbf{I} + \mathbf{D}^{\mathrm{Pro}*}) + (2\pi\mathbf{I} - \mathbf{D}^{\mathrm{Sol}})\mathbf{S}^{\mathrm{Pro}}]\mathbf{A}^{-1}\mathbf{q}_{\mathbf{s}'}{}^{\mathrm{bound}} = \mathbf{S}^{\mathrm{Sol}}\mathbf{E}_{\mathbf{s}'} - (2\pi\mathbf{I} - \mathbf{D}^{\mathrm{Sol}})\mathbf{V}_{\mathbf{s}'} \quad \text{(A2)}$$

where $\mathbf{V}_{\mathbf{s}'}$ and $\mathbf{E}_{\mathbf{s}'}$ are the analogs to $\mathbf{V}_\rho$ and $\mathbf{E}_\rho$ in eq A1, but calculated from a unitary point charge placed in $\mathbf{s}'$ inside an infinite, homogeneous medium characterized by the Green's function $G^{\mathrm{pro}}(\mathbf{r}, \mathbf{r}')$. The matrices $\mathbf{S}^{\mathrm{Pro}}$ and $\mathbf{D}^{\mathrm{Pro}}$ are built from $G^{\mathrm{pro}}(\mathbf{r}, \mathbf{r}')$, while $\mathbf{S}^{\mathrm{Sol}}$ and $\mathbf{D}^{\mathrm{Sol}}$ are built from $G^{\mathrm{sol}}(\mathbf{r}, \mathbf{r}')$, the Green's function proper for the solvent medium surrounding the protein. As discussed already, for the calculations including the tip and the substrate in the system, $G^{\mathrm{sol}}(\mathbf{r}, \mathbf{r}')$ contains image terms that take care of the boundary conditions at the solvent/tip and solvent/substrate interfaces, which in turn do not have to be considered explicitly.

Once eq A2 has been solved for each value of $\mathbf{s}'$, $G^{\mathrm{bound}}(\mathbf{s}, \mathbf{s}')$ (and thus, $G^{\mathrm{out}}(\mathbf{s}, \mathbf{s}') = G^{\mathrm{bound}}(\mathbf{s}, \mathbf{s}') + G^{\mathrm{pro}}(\mathbf{s}, \mathbf{s}')$) is known for all the tessera pairs $\mathbf{s}$, $\mathbf{s}'$, the matrices $\mathbf{S}^{\mathrm{Out}}$ and $\mathbf{D}^{\mathrm{Out}}$ needed in eq A1 can then be built, and eq A1 can eventually be solved with standard linear algebra techniques, giving $\mathbf{q}$. From $\mathbf{q}$, the wanted $V[\rho_{\mathrm{R/P}}]$ is finally calculated.

The procedure presented here has been implemented in a local code interfaced with GAMESS. Typical numbers of tesserae used in the calculations were around 1500 per protein for the protein/solvent boundary and 700 per cavity for the cavity/protein boundary.

Acknowledgment. The author thanks Rosa Di Felice and Elisa Molinari for critical reading of previous versions of the manuscript, and Paolo Facci and Andrea Alessandrini for many useful discussions. Funding was provided by the INFM Parallel Computing Committee, by the EU (IST-FET-SAMBA), and by MIUR (FIRB-NOMADE).

References and Notes

(1) Solomon, E. I.; Szilagyi, R. K.; DeBeer, G. S.; Basumallick, L. *Chem. Rev.* **2004**, *104*, 419.

(2) Vijgenboom, E.; Busch, J. E.; Canters, G. W. *Microbiology* **1997**, *143*, 2853.

(3) Rinaldi, R.; Biasco, A.; Maruccio, G.; Cingolani, R.; Alliata, D.; Andolfi, L.; Facci, P.; De Rienzo, F.; Di Felice, R.; Molinari, E. *Adv. Mater*. **2002**, *14*, 1453.

(4) Friis, E. P.; Andersen, J. E. T.; Kharkats, Y. I.; Kuznetsov, A. M.; Nichols, R. J.; Zhang, J. D.; Ulstrup, J. *Proc. Natl. Acad. Sci. U.S.A.* **1999**, *96*, 1379.

(5) Chi, Q.; Zhang, J.; Nielsen, J. U.; Friis, E. P.; Chorkendorff, I.; Canters, G. W.; Andersen, J. E. T.; Ulstrup, J. *J. Am. Chem. Soc.* **2000**, *122*, 4047.

(6) Alessandrini, A.; Gerunda, M.; Canters, G. W.; Verbeet, M. Ph; Facci, P. *Chem. Phys. Lett.* **2003**, *376*, 625.

(7) (a) Olsson, M. H. M.; Hong, G.; Warshel, A. *J. Am. Chem. Soc.* **2003**, *125*, 5025. (b) Simonson, T. *Proc. Natl. Acad. Sci. U.S.A.* **2002**, *99*, 6544. (c) Zhou, H.-X. *J. Am. Chem. Soc.* **1994**, *116*, 10362.

(8) (a) Schmickler, W. *Surf. Sci.* **1993**, *295*, 43. (b) Friis, E. P.; Kharkats, Y. I.; Kuznetsov, A. M.; Ulstrup, J. *J. Phys. Chem. A* **1998**, *102*, 7851. (c) Kuznetsov, A. M.; Ulstrup, J. *J. Phys. Chem. A* **2000**, *104*, 11531.

(9) Ryde, U.; Olsson, M. H. M. *Int. J. Quantum Chem.* **2001**, *81*, 335.

(10) van Amsterdam, I. M. C.; Ubbink, M.; Einsle, O.; Messerschmidt, A.; Merli, A.; Cavazzini, D.; Rossi, G. L.; Canters, G. W. *Nat. Struct. Bio.* **2002**, *9*, 48.

(11) Nar, H.; Messerschmidt, A.; Huber, R.; van de Kamp, M.; Canters, G. W. *J. Mol. Biol.* **1991**, *221*, 765.

(12) (a) Cancès, E.; Mennucci, B.; Tomasi, J. *J. Chem. Phys.* **1997**, *107*, 3031. (b) Cancès, E.; Mennucci, B.; Tomasi, J. *J. Phys. Chem. B* **1997**, *101*, 10506. (c) Cancès, E.; Mennucci, B. *J. Math. Chem.* **1998**, *23*, 309.

(13) Miertus, S.; Scrocco, E.; Tomasi, J. *Chem. Phys.* **1981**, *55*, 117.

(14) Schmidt, M. W.; Baldridge, K. K.; Boatz, J. A.; Elbert, S. T.; Gordon, M. S.; Jensen, J. H.; Koseki, S.; Matsunaga, N.; Nguyen, K. A.; Su, S. J.; Windus, T. L.; Dupuis, M.; Montgomery, J. A. *J. Comput. Chem.* **1993**, *14*, 1347.

(15) Tomasi, J.; Cammi, R.; Mennucci, B.; Cappelli, C.; Corni, S. *Phys. Chem. Chem. Phys*. **2002**, *4*, 5697.

(16) Corni, S.; De Rienzo, F.; Di Felice, R.; Molinari, E. *Int. J. Quantum Chem.*, in press.

(17) Luque, F. J.; Zhang, Y.; Aleman, C.; Bachs, M.; Gao, J.; Orozco, M. *J. Phys. Chem.* **1996**, *100*, 4269.

(18) Tomasi, J.; Persico, M. *Chem. Rev.* **1994**, *94*, 2027.

(19) Pascual-Ahuir, J. L.; Silla, E.; Tuñon, I. *J. Comput. Chem.* **1994**, *15*, 1127.

(20) Frisch, M. J.; Trucks, G. W.; Schlegel, H. B.; Scuseria, G. E.; Robb, M. A.; Cheeseman, J. R.; Zakrzewski, V. G.; Montgomery, J. A., Jr.; Stratmann, R. E.; Burant, J. C.; Dapprich, S.; Millam, J. M.; Daniels, A. D.; Kudin, K. N.; Strain, M. C.; Farkas, O.; Tomasi, J.; Barone, V.; Cossi, M.; Cammi, R.; Mennucci, B.; Pomelli, C.; Adamo, C.; Clifford, S.; Ochterski, J.; Petersson, G. A.; Ayala, P. Y.; Cui, Q.; Morokuma, K.; Malick, D. K.; Rabuck, A. D.; Raghavachari, K.; Foresman, J. B.; Cioslowski, J.; Ortiz, J. V.; Stefanov, B. B.; Liu, G.; Liashenko, A.; Piskorz, P.; Komaromi, I.; Gomperts, R.; Martin, R. L.; Fox, D. J.; Keith, T.; Al-Laham, M. A.; Peng, C. Y.; Nanayakkara, A.; Gonzalez, C.; Challacombe, M.; Gill, P. M. W.; Johnson, B. G.; Chen, W.; Wong, M. W.; Andres, J. L.; Head-Gordon, M.; Replogle, E. S.; Pople, J. A. *Gaussian 98*; Gaussian, Inc.: Pittsburgh, PA, 1998.

(21) Kornyshev, A. A. In *The Chemical Physics of Solvation*; Dogonadze, R., Kámál, E., Kornyshev, A. A., Ulstrup, J., Eds.; Elsevier: Amsterdam, 1985; Part A, p 85, eq 3.13.

(22) (a) Bopp, P. A.; Kornyshev, A. A.; Sutmann, G. *Phys. Rev. Lett.* **1996**, *76*, 1280. (b) Kornyshev, A. A.; Kuznetsov, A. M.; Ulstrup, J.; Stimming, U. *J. Phys. Chem. B* **1997**, *101*, 5917. (c) Perng, B.-C.; Ladanyi, B. M. *J. Chem. Phys.* **1999**, *110*, 6389.

(23) (a) LeBard, D. N.; Lilichenko, M.; Matyushov, D. V.; Berlin, Y. A.; Ratner, M. A. *J. Phys. Chem. B* **2003**, *107*, 14509. (b) Matyushov, D. V. *J. Chem. Phys.* **2004**, *120*, 7532.

(24) Basilevsky, M. V.; Parsons, D. F. *J. Chem. Phys.* **1998**, *108*, 9114.

(25) Liu, Y.-P.; Newton, M. D. *J. Phys. Chem*. **1995**, *99*, 12382.

(26) Cammi, R.; Tomasi, J. *J. Comput. Chem.* **1995**, *16*, 1449.

(27) (a) Zhou, H.-X. *J. Chem. Phys.* **1996**, *105*, 3726. (b) Höfinger, S.; Simonson, T. *J. Comput. Chem.* **2001**, *22*, 290.

(28) Marcus, R. A. *J. Chem. Phys.* **1956**, *24*, 967.

(29) Marcus, R. A. *J. Chem. Phys.* **1956**, *24*, 979.

(30) Cammi, R.; Tomasi, J. *Int. J. Quantum Chem.* **1995**, *Suppl. 29*, 465.

(31) Cappeli, C.; Corni, S.; Cammi, R.; Mennucci, B.; Tomasi, J. *J. Chem. Phys.* **2000**, *113*, 11270.

(32) (a) Di Bilio, A. J.; Hill, M. G.; Bonander, N.; Karlsson, B. G.; Villahermosa, R. M.; Malmström, B. G.; Winkler, J. R.; Gray, H. B. *J. Am. Chem. Soc.* **1997**, *119*, 9921. (b) Gray, H. B.; Malmström, B. G.; Williams, R. J. P. *J. Biol. Inorg. Chem*. **2000**, *5*, 551.

(33) Gerischer, H. *Adv. Electrochem. Electrochem. Eng.* **1961**, *1*, 139.

(34) Bard, A. J.; Faulkner, L. R. *Electrochemical Methods*; Wiley: New York, 2001.

(35) Facci, P. Private communications.

(36) Teschke, O.; Ceotto, G.; de Souza, E. F. *Phys. Chem. Chem. Phys.* **2001**, *3*, 3761.

(37) (a) Corni, S.; Tomasi, J. *J. Chem. Phys.* **2002**, *117*, 7266. (b) Corni, S.; Tomasi, J. *J. Chem. Phys.* **2003**, *118*, 6481. (c) Andreussi, O.; Corni, S.; Mennucci, B.; Tomasi, J. *J. Chem. Phys.* **2004**, *121*, 10190.